Quantum properties of nonclassical states generated by an optomechanical system with catalytic quantum scissors

Heng-Mei Li(李恒梅)[1,†], Bao-Hua Yang(杨保华)[1], Hong-Chun Yuan(袁洪春)[2], and Ye-Jun Xu(许业军)[3]

[1] *School of Information Engineering, Changzhou Vocational Institute of Mechatronic Technology, Changzhou* 213164, *China*
[2] *School of Electrical and Information Engineering, Changzhou Institute of Technology, Changzhou* 213032, *China*
[3] *School of Mechanical and Electronic Engineering, Chizhou University, Chizhou* 247000, *China*

(Received 22 March 2022; revised manuscript received 4 May 2022; accepted manuscript online 23 May 2022)

A scheme is proposed to investigate the non-classical states generated by a quantum scissors device (QSD) operating on the the cavity mode of an optomechanical system. When the catalytic QSD acts on the cavity mode of the optomechanical system, the resulting state contains only the vacuum, single-photon and two-photon states depending upon the coupling parameter of the optomechanical system as well as the transmission coefficients of beam splitters (BSs). Especially, the output state is just a class of multicomponent cat state truncations at time $t = 2\pi$ by choosing the appropriate value of coupling parameter. We discuss the success probability of such a state and the fidelity between the output state and input state via QSD. Then the linear entropy is used to investigate the entanglement between the two subsystems, finding that QSD operation can enhance their entanglement degree. Furthermore, we also derive the analytical expression of the Wigner function (WF) for the cavity mode via QSD and numerically analyze the WF distribution in phase space at time $t = 2\pi$. These results show that the high non-classicality of output state can always be achieved by modulating the coupling parameter of the optomechanical system as well as the transmittance of BSs.

Keywords: optomechanical system, quantum scissors device, quantum state engineering, linear entropy

PACS: 42.50.Dv, 42.50.Pq, 03.65.Ta **DOI:** 10.1088/1674-1056/ac7206

1. Introduction

In recent decades, physicists have devoted themselves to preparation and manipulation of highly non-classical quantum states in order to meet requirements of quantum information processing.[1–3] Among them, many protocols using non-Gaussian operations such as photon addition,[4–8] photon substraction,[9–11] and various combinations[12–14] have been proposed to achieve novel non-classical quantum states, which is one of most effective methods. Agarwal and Tara first introduced the photon-added coherent state obtained by repeated applications of the creation operator on a coherent state, exhibiting both higher-order squeezing and sub-Poissonian characteristics.[4] In addition, these non-Gaussian operations can also enhance the nonlocality and increase the degree of entanglement of quantum states,[15,16] which was then used to improve the fidelity of quantum teleportation,[17] the performance of the quantum key distribution,[18] and quantum metrology.[19]

Another effective scheme is known to quantum truncation based on quantum scissors device (QSD) proposed by Pegg *et al.*,[20] which enables generation of superposition of vacuum and single-photon states by truncating a coherent state. In the above scheme, beam splitters (BSs) and condition measurements were mainly utilized. Indeed, QSD is just a non-local phenomenon depending on entanglement where there was no light traveled from the input mode to the output mode. The basic idea of QSD had been extended to generate not only qubits but also qutrits and qudits of any dimension.[21–26] Later, the QSD scheme was generalized to a non-deterministic noiseless amplifier[27] and also applied as a teleportation device for superposition states.[28,29] To extend the above-mentioned works, thermal state truncation was proposed via QSD to generate a mixture of vacuum and single-photon states.[30] By applying QSDs to both modes of the two-mode squeezed vacuum state (TMSVS), the resulting state was the entangled state composed of the twin vacuum and the twin single-photon, which can realize the enhance of entanglement and the improvement of the fidelity of teleportation.[31] Zhang *et al.* presented a slight modification to propose a catalytic QSD[32] and a displacement-based QSD[33] to truncate the input coherent state, indicating that the output state is a highly non-classical quantum state. In addition, we adopted the basic idea of QSD to generate the finite-dimensional quantum states including the single-mode case and the two-mode case.[34] More interestingly, QSD can be placed at the receiving end of the continuous-variable quantum key distribution in order to lengthen the transmission distance.[35] These truncated states exhibit various interesting properties that may be a subject of a broad range of investigation in the field of quantum optics.

On the other hand, it is well known that an optomechanical system is a very useful platform for quantum state engineering.[36–40] For example, Mancini *et al.* synthesized Schrödinger-cat states of cavity field by means of the optome-

[†]Corresponding author. E-mail: lihengm@ustc.edu.cn

© 2023 Chinese Physical Society and IOP Publishing Ltd

chanical system.[41] In Ref. [42], the authors utilized an optomechanical system to generate a large variety of nonclassical states of both the cavity field and the mechanical mode, including entangled states of two or more cavity modes.[43] A coupled optomechanical system can also be used to obtain squeezing states of mechanical mode.[44] A question arises naturally: How do the resulting nonclassical states effect when operating QSD on the dynamics of the optomechanical system? So far as we know, this question has not been clearly investigated in the literature to date.

In order to clearly understand the above influence, here we propose a scheme to generate new nonclassical quantum states by operating QSD on the cavity mode of the optomechanical system, where two single-photons are used to be in input modes of BS1 and perfect photondetector in output modes of BS2 registers one photoncount (see Fig. 1 in detail). The organization of this paper is as follows. In Section 2, we first briefly review the theoretical models of the optomechanical system and the catalytic QSD with single photon input and single photon detection. In addition, we also give the corresponding equivalent operator of catalytic QSD depending upon the transmission coefficients of BSs. In Section 3, under the catalytic QSD, the main focus is the fidelity between the input state and the output state to assess the influence of the optomechanical system. In Section 4, we mainly discuss linear entropy of the cavity mode to numerically evaluate how QSD operation can effect the degree of entanglement between the cavity field and the mechanical oscillator. In Section 5, the nonclassical characteristics of the output state are analyzed in detail by means of the Wigner function (WF). Finally, the main results are summarized in Section 6.

2. Theoretical model

We first theoretically introduce a scheme to generate the new nonclassical states by operating QSD on the cavity mode as illustrated in Fig. 1.

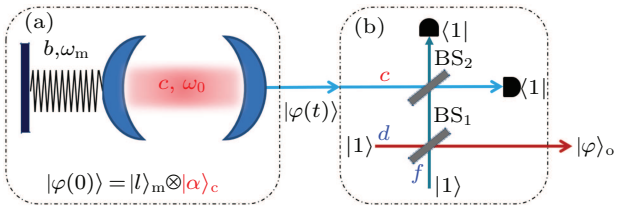


Fig. 1. Schematic diagram of generating the non-classical state $|\psi\rangle_{\rm o}$ via QSD based on BSs and conditional measurements, where two single-photons $|1\rangle$ are used to be in input modes of BS$_1$ and perfect photodetector in output modes of BS$_2$ all registers one photocount.

2.1. The optomechanical system

To begin with, we briefly review the isolated optomechanical system of a cavity field and a movable mirror. As shown in Fig. 1, the movable mirror is a quantum harmonic oscillator with frequency $\omega_{\rm m}$ and annihilation operator denoted by b, interacting with a cavity field mode of frequency ω_0 and annihilation operator denoted by c. The relevant Hamiltonian is[41]

$$H=\hbar\omega_0 c^{\dagger}c+\hbar\omega_{\rm m}b^{\dagger}b-\hbar\chi c^{\dagger}c(b+b^{\dagger}), \tag{1}$$

where $\chi=\omega_0\sqrt{\hbar/2m\omega_{\rm m}}/L$ is the coupling constant between the modes, L and m are the length of the cavity and the mass of movable mirror, respectively. Let us assume that the cavity field is initially in coherent state $|\alpha\rangle_{\rm c}=\mathrm{e}^{-|\alpha|^2/2}\sum_{n=0}^{\infty}\alpha^n/\sqrt{n!}\,|n\rangle_{\rm c}$ and the mechanical resonator is in number state $|l\rangle_{\rm m}$, thus the initial state at time $t=0$ is written as $|\varphi(0)\rangle=|\alpha\rangle_{\rm c}|l\rangle_{\rm m}$. Then the state of the optomechanical system with the time evolution is given by[42]

$$\begin{aligned}|\varphi(t)\rangle&=\mathrm{e}^{-|\alpha|^2/2}\sum_{n=0}^{\infty}\frac{\alpha^n}{\sqrt{n!}}\mathrm{e}^{\mathrm{i}k^2n^2(t-\sin t)}|n\rangle_{\rm c}D(kn\eta)|l\rangle_{\rm m}\\&=\sum_{n=0}^{\infty}C_n(\alpha)|n\rangle_{\rm c}D(kn\eta)|l\rangle_{\rm m},\end{aligned} \tag{2}$$

where $C_n(\alpha)\equiv\frac{\mathrm{e}^{-|\alpha|^2/2}\alpha^n}{\sqrt{n!}}\mathrm{e}^{\mathrm{i}k^2n^2(t-\sin t)}$, $k=\chi/\omega_{\rm m}$ is the scaled coupling parameter, $D(\beta)=\exp\left(\beta b^{\dagger}-\beta^{*}b\right)$ denotes the displacement operator with $\eta=1-\mathrm{e}^{-\mathrm{i}t}$, and the scaled time t is equal to the time multiplied by $\omega_{\rm m}$.

It is easily obtained from Eq. (2) that when $t=2\pi$ and $\eta=0$, the mirror returns to its original state and the state of cavity field turns into

$$|\xi\rangle_{\rm c}\equiv\mathrm{e}^{-|\alpha|^2/2}\sum_{n=0}^{\infty}\frac{\alpha^n}{\sqrt{n!}}\mathrm{e}^{\mathrm{i}2\pi k^2n^2}|n\rangle_{\rm c}. \tag{3}$$

In addition, depending on the value of the parameter k, the state $|\xi\rangle_{\rm c}$ can be made equivalent to a variety of multicomponent cat states at time $t=2\pi$. For example, for $k=1/2$, we obtain the two-component Schrödinger cat state

$$|\xi_2\rangle_{\rm c}=\mathrm{e}^{-|\alpha|^2/2}\left[\left(\frac{1+\mathrm{i}}{2}\right)|\alpha\rangle_{\rm c}+\left(\frac{1-\mathrm{i}}{2}\right)|-\alpha\rangle_{\rm c}\right]. \tag{4}$$

For $k=1/\sqrt{6}$ and $k=1/(2\sqrt{2})$, we obtain the three-component and four-component cat states (not normalized) as follows:

$$|\xi_3\rangle_{\rm c}=h_1|-\alpha\rangle_{\rm c}+h_2\left|\alpha\mathrm{e}^{\mathrm{i}\frac{\pi}{3}}\right\rangle_{\rm c}+h_3\left|\alpha\mathrm{e}^{-\mathrm{i}\frac{\pi}{3}}\right\rangle_{\rm c}, \tag{5}$$

$$|\xi_4\rangle_{\rm c}=\frac{\mathrm{e}^{\mathrm{i}\pi/4}}{2}(|\alpha\rangle_{\rm c}-|-\alpha\rangle_{\rm c})+\frac{1}{2}(|\mathrm{i}\alpha\rangle_{\rm c}+|-\mathrm{i}\alpha\rangle_{\rm c}), \tag{6}$$

where $h_2=h_3=\left(1+\mathrm{e}^{\mathrm{i}\pi/3}\right)/[2[1+\cos(\pi/3)]]$ and $h_1=1-2h_2$. Thus, by adjusting the ratio of the coupling and the mirror frequency and thereby varying k, one can in principle obtain all these types of cat states at time $t=2\pi$.

2.2. Quantum scissors device

The schematic diagram of QSD proposed by Pegg *et al.*[20] consists of two BSs and two photon counting detectors, as shown in Fig. 1. The input modes of the setup are denoted as c, d, and f, and their corresponding creation operators are $c^\dagger$, $d^\dagger$, and $f^\dagger$, respectively. Two single-photon states at auxiliary input modes d and f successively interact with two BSs $B_1 = \exp\left[\theta_1\left(d^\dagger f - f^\dagger d\right)\right]$ and $B_2 = \exp\left[\theta_2\left(c^\dagger f - f^\dagger c\right)\right]$, where $t_j = \cos\theta_j$ and $r_j = \sin\theta_j$ $(j = 1, 2)$ are transmission coefficient and reflection coefficient of BSs. When perfect photodetectors at output modes c and f of BS_2 register only one photocount, respectively, the output state $|\psi\rangle_o$ at output mode d of BS_1 is given by

$$\begin{aligned}|\psi\rangle_o &= \frac{1}{\sqrt{p_s}}\,{}_c\langle 1|_f\langle 1|B_2B_1|1\rangle_d|1\rangle_f|\varphi\rangle_{in}\\ &= \frac{1}{\sqrt{p_s}}\hat{O}|\varphi\rangle_{in},\end{aligned} \tag{7}$$

where the normalization factor p_s represents the success probability heralded by the detection of one photoncount at the modes c and f of BS_2, and $\hat{O} = {}_c\langle 1|_f\langle 1|B_2B_1|1\rangle_d|1\rangle_f$ is derived as

$$\begin{aligned}\hat{O} &= -2\Gamma_0|0\rangle_{dc}\langle 0| + \Gamma_1|1\rangle_{dc}\langle 1| - 2\Gamma_0|2\rangle_{dc}\langle 2|\\ &= -2\Gamma_0|0\rangle_{dc}\langle 0| + \Gamma_1 d^\dagger|0\rangle_{dc}\langle 0|c - \Gamma_0 d^{\dagger 2}|0\rangle_{dc}\langle 0|c^2\end{aligned} \tag{8}$$

with $\Gamma_0 = t_1t_2r_1r_2$ and $\Gamma_1 = (r_1^2 - t_1^2)(r_2^2 - t_2^2)$. Especially, when $T_1 = t_1^2 = 0.5$ (or $T_2 = t_2^2 = 0.5$) leading to $\Gamma_1 = 0$, and $T_1 = t_1^2 = 1$ (or $T_2 = t_2^2 = 1$) leading to $\Gamma_0 = 0$, the operator $\hat{O}$ turns into $\hat{O} \to -2\Gamma_0|0\rangle_{dc}\langle 0| - 2\Gamma_0|2\rangle_{dc}\langle 2|$ and $\hat{O} \to \Gamma_1|1\rangle_{ab}\langle 1|$, respectively. The more detailed calculations can be seen in Ref. [35]. It is shown from Eqs. (7) and (8) that QSD operation truncates an arbitrary input state $|\varphi\rangle_{in}$ into the quantum state with the vacuum, one-photon and two-photon components. Obviously, when the state of cavity field above is performed by QSD, namely, $|\xi\rangle_c$ as the input state of QSD, according to Eqs. (2) and (8) the output state $|\psi\rangle_o$ is obtained as follows:

$$\begin{aligned}|\psi\rangle_o = \frac{1}{\sqrt{p_s}}\big(&-2\Gamma_0C_0(\alpha)|0\rangle_d|l\rangle_m + \Gamma_1C_1(\alpha)D(k\eta)|1\rangle_d|l\rangle_m\\ &-2\Gamma_0C_2(\alpha)D(2k\eta)|2\rangle_d|l\rangle_m\big).\end{aligned} \tag{9}$$

Such state is modulated by adjusting the parameter k and time t of the optomechanical system as well as the transmittance of BSs, generating a wide range of nonclassical phenomena. Especially, at time $t = 2\pi$, the nonclassical state of the cavity field at output mode d is given by

$$\begin{aligned}|\psi'\rangle_o = \frac{e^{-|\alpha|^2/2}}{\sqrt{p_s}}\big(&-2\Gamma_0|0\rangle_d + \alpha\Gamma_1 e^{i2\pi k^2}|1\rangle_d\\ &-\sqrt{2}\alpha^2\Gamma_0 e^{i8\pi k^2}|2\rangle_d\big).\end{aligned} \tag{10}$$

When $k = 0.5$, the Schrödinger cat state was operated by quantum scissor, discussed in detail in Ref. [26].

2.3. Detection probability

Next, before analyzing the nonclassical characteristics of the output state $|\psi\rangle_o$, it is necessary to derive the explicit expression of the normalization factor p_s, i.e., the success probability of such a state in Eq. (9). According to the completeness of quantum state, p_s can be directly calculated by

$$p_s = e^{-|\alpha|^2}\left(4\Gamma_0^2 + |\alpha|^2\Gamma_1^2 + 2|\alpha|^4\Gamma_0^2\right), \tag{11}$$

which is just the specific expression of the detection probability of the output state $|\psi\rangle_o$. It is seen from Eq. (11) that the detection probability p_s is related to the transmittance T_1, T_2 of two BSs and the amplitude $|\alpha|$ of initial coherent state, independent of parameter k and time t. According to Eq. (11), we plot the detection probability of $|\psi\rangle_o$ in Fig. 2 as a function of the coherent amplitude $|\alpha|$ and the transmissivity $T_2 = t_2^2$ for several different cases. When $T_1 = 1$ and $T_2 = 1$, leading to $\Gamma_0 = 0$ and $\Gamma_1 = 1$, $p_s = e^{-|\alpha|^2}|\alpha|^2$ (see the blue solid line in Fig. 2(a)). We see that for the case of $T_1 \neq 1$ and $T_2 \neq 1$ the success probability all decreases with the increasing amplitude $|\alpha|$ in Fig. 2(a) and for a given $|\alpha| = 0.5$ and T_1, the curves in Fig. 2(b) are symmetric about $T_2 = 0.5$, and the corresponding maximum value increases with the increasing T_1 ($T_1 < 0.5$).

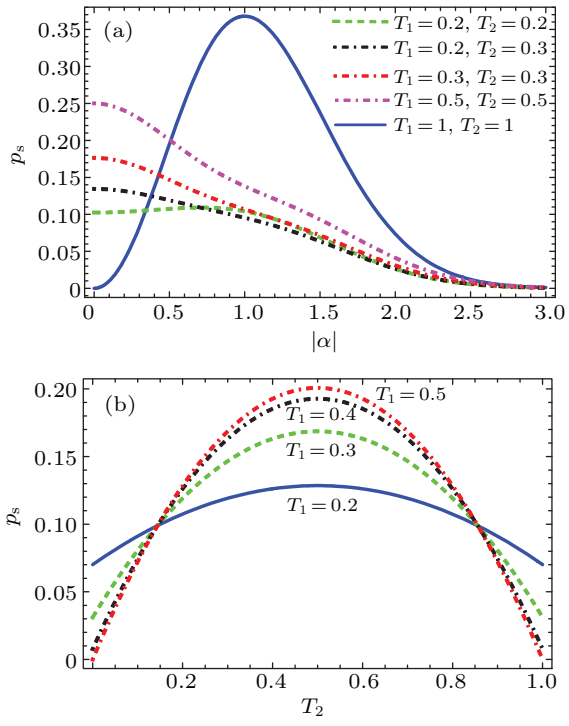


Fig. 2. Success probability of such a state $|\psi\rangle_o$ as a function of (a) the coherent amplitude $|\alpha|$ for several different T_1 and T_2 and (b) T_2 for several different T_1 at fixed $|\alpha| = 0.5$, respectively.

3. Fidelity

In this section, under the catalytic QSD, we introduce the fidelity between the input state $|\varphi\rangle_{in}$ and the output state $|\psi\rangle_o$ to assess the influence of the optomechanical system, which

is defined as $F = |_{\rm in}\langle\varphi\,|\psi\rangle_{\rm o}|^2$.[26,45] Thus, using Eqs. (2) and (9), the fidelity F can be calculated by

$$\begin{aligned} F &= \frac{1}{p_{\rm s}}\left(-2\Gamma_0|C_0(\alpha)|^2+\Gamma_1|C_1(\alpha)|^2-2\Gamma_0|C_2(\alpha)|^2\right)^2 \\ &= \frac{1}{p_{\rm s}}\,{\rm e}^{-2|\alpha|^2}\left(-2\Gamma_0+\Gamma_1|\alpha|^2-\Gamma_0|\alpha|^4\right)^2. \end{aligned} \tag{12}$$

It is found from Eq. (12) that the fidelity is also independent of the scaled coupling parameter k and time t.

To see clearly the variation of the fidelity, using Eq. (12) we plot the fidelity F between the output state and input state in the QSD as a function of amplitude $|\alpha|$ or transmissivities T_1 and T_2 for several different cases, respectively, as shown in Fig. 3. It is clear in Fig. 3(a) that the fidelity can be close to 1 for a small amplitude $|\alpha|$ with given transmissivities T_1 and T_2, and monotonously decreases with the increasing $|\alpha|$ for high transmissivities T_2 (e.g., $T_2 = 0.4$ or $T_2 = 0.5$). However, for low transmissivities T_2 (e.g., $T_2 = 0.1$ or $T_2 = 0.15$) it firstly decreases from 1 to zero and then increases to the maximum value and subsequently tends to zero with the increasing $|\alpha|$. For the case of $T_1 = T_2$ (see Fig. 3(b)), the fidelity is symmetrically distributed with $T_1 = T_2 = 0.5$ (i.e., 50:50 beam splitter) and the maximum value decreases with the increasing $|\alpha|$. In fact, when $T_2 = 0.5$ (or $T_1 = 0.5$), leading to $\Gamma_1 = 0$, we obtain that the fidelity can be simplified to ${\rm e}^{-|\alpha|^2}\left(\frac{1}{2}|\alpha|^4+1\right)$, which is independent of T_1 (or T_2), as shown in Figs. 3(c) and 3(d). When $|\alpha| = 1.0$ and 1.5, F is approximately equal to 0.55 and 0.37, respectively. In addition, for a given $|\alpha|$, there exists a common intersection at $T_1 = 0.5$ ($T_2 = 0.5$) for several different T_2 (T_1), and T_1 dependence of the fidelity is the same as T_2. These results illustrate that the high fidelity can be achieved by adjusting the transmissivity and amplitude.

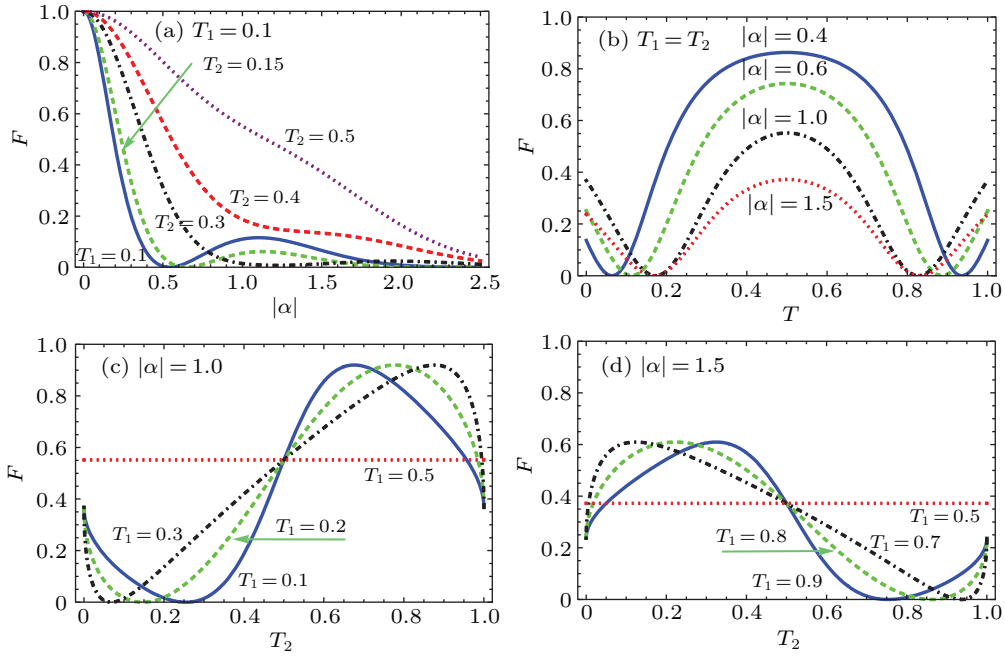


Fig. 3. Fidelity F between the output state and input state in the quantum scissor device as a function of amplitude $|\alpha|$ or transmissivities T_1 and T_2 for several different cases, where (a) at fixed $T_1 = 0.1$, (b) $T = T_1 = T_2$, (c) at fixed $|\alpha| = 1.0$, and (d) at fixed $|\alpha| = 1.5$.

4. Linear entropy

In this section, we discuss whether QSD can affect the degree of entanglement between the cavity field and the mechanical oscillator by evaluating linear entropy[46]

$$S = 1 - {\rm Tr}(\rho_{\rm c}^2(t)), \tag{13}$$

where $\rho_{\rm c}(t)$ is the reduced density matrix of the cavity mode. Thus, for the initial optomechanical system, using Eq. (2) the partial trace of density matrix $\rho(t) = |\varphi(t)\rangle\langle\varphi(t)|$ over the mechanical mode is expressed as

$$\begin{aligned} \rho_i(t) &= {\rm Tr}_{\rm m}(|\varphi(t)\rangle\langle\varphi(t)|) \\ &= \sum_{n,n'=0}^{\infty} C_n(\alpha)C_{n'}^*(\alpha)\Pi_l(k(n'-n)\eta)\,|n\rangle_{\rm c}\langle n'|, \end{aligned} \tag{14}$$

and linear entropy S_i of the cavity mode can also be obtained by

$$\begin{aligned} S_i &= 1-{\rm Tr}(\rho_i^2(t)) \\ &= 1-\sum_{n,n'=0}^{\infty}|C_n(\alpha)C_{n'}(\alpha)|^2\left[\Pi_l(k(n'-n)\eta)\right]^2. \end{aligned} \tag{15}$$

Here, we have used the following formula:

$$D(\alpha)D(\beta) = D(\alpha+\beta)\,{\rm e}^{\frac{1}{2}(\beta^*\alpha-\alpha^*\beta)}, \tag{16}$$

$$\Pi_l(\beta) \equiv {}_{\rm m}\langle l|D(\beta)|l\rangle_{\rm m} = {\rm e}^{-\frac{|\beta|^2}{2}}L_l\left(|\beta|^2\right) \tag{17}$$

with the Laguerre polynomials $L_n(x) = \sum_{l=0}^{n}\binom{n}{l}\frac{(-x)^l}{l!}$.

Similarly, when operating QSD, we obtain from Eq. (9)

that

$$\rho_{\rm o}(t) = {\rm Tr}_{\rm m}\left(|\psi\rangle_{\rm o}\langle\psi|\right) = \frac{1}{p_{\rm s}}\begin{pmatrix} \kappa_{00}|0\rangle_{\rm d}\langle 0| + \kappa_{01}^{*}|1\rangle_{\rm d}\langle 0| + \kappa_{02}^{*}|2\rangle_{\rm d}\langle 0| \\ +\kappa_{01}|0\rangle_{\rm d}\langle 1| + \kappa_{11}|1\rangle_{\rm d}\langle 1| + \kappa_{12}^{*}|2\rangle_{\rm d}\langle 1| \\ +\kappa_{02}|0\rangle_{\rm d}\langle 2| + \kappa_{12}|1\rangle_{\rm d}\langle 2| + \kappa_{22}|2\rangle_{\rm d}\langle 2| \end{pmatrix}, \quad (18)$$

where

$$\begin{aligned} \kappa_{00} &= 4\Gamma_0^2|C_0(\alpha)|^2, \\ \kappa_{01} &= -2\Pi_l(k\eta)\Gamma_0\Gamma_1 C_0(\alpha)C_1^{*}(\alpha), \\ \kappa_{11} &= \Gamma_1^2|C_1(\alpha)|^2, \\ \kappa_{02} &= 4\Pi_l(2k\eta)\Gamma_0^2 C_0(\alpha)C_2^{*}(\alpha), \\ \kappa_{22} &= 4\Gamma_0^2|C_2(\alpha)|^2, \\ \kappa_{12} &= -2\Pi_l(k\eta)\Gamma_0\Gamma_1 C_1(\alpha)C_2^{*}(\alpha). \end{aligned} \quad (19)$$

Substituting Eq. (18) into Eq. (13) yields

$$S_{\rm c} = 1 - p_{\rm s}^{-2}\left(|\kappa_{00}|^2 + 2|\kappa_{01}|^2 + 2|\kappa_{02}|^2 + 2|\kappa_{12}|^2 + |\kappa_{11}|^2 + |\kappa_{22}|^2\right), \quad (20)$$

which is just the analytical expression of linear entropy for the cavity mode. Generally, the greater the linear entropy is, the stronger the entanglement is.

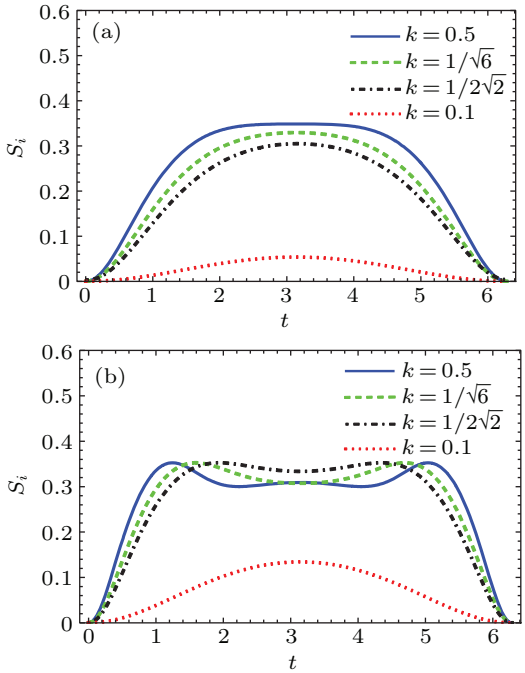


Fig. 4. Linear entropy S_i of the cavity mode without operating quantum scissors as a function of time t for several different values of the scaled coupling parameter k with $|\alpha| = 0.5$, where the initial number state is (a) $|1\rangle_{\rm m}$ and (b) $|4\rangle_{\rm m}$ in the mechanical mode.

According to Eq. (15), we plot the linear entropy S_i of the cavity mode before operating quantum scissors as a function of time t for several different values of the scaled coupling parameter k in Fig. 4. It is seen that the degree of entanglement of the cavity field with the mechanical oscillator all are symmetric about $t = \pi$. For the case of the initial number state $|1\rangle_{\rm m}$ in Fig. 4(a), the degree of entanglement increases from zero to the maximum value at $t = \pi$, where the maximum value decreases with the decreasing parameter k, and subsequently decreases to zero at $t = 2\pi$. After a time $t = 2\pi$, the mirror returns to its original state and the entanglement vanishes gradually, as is expected. However, with the increasing number state the degree of entanglement clearly shows obvious oscillation behavior and their maximum values are not located at $t = \pi$ (see Fig. 4(b)).

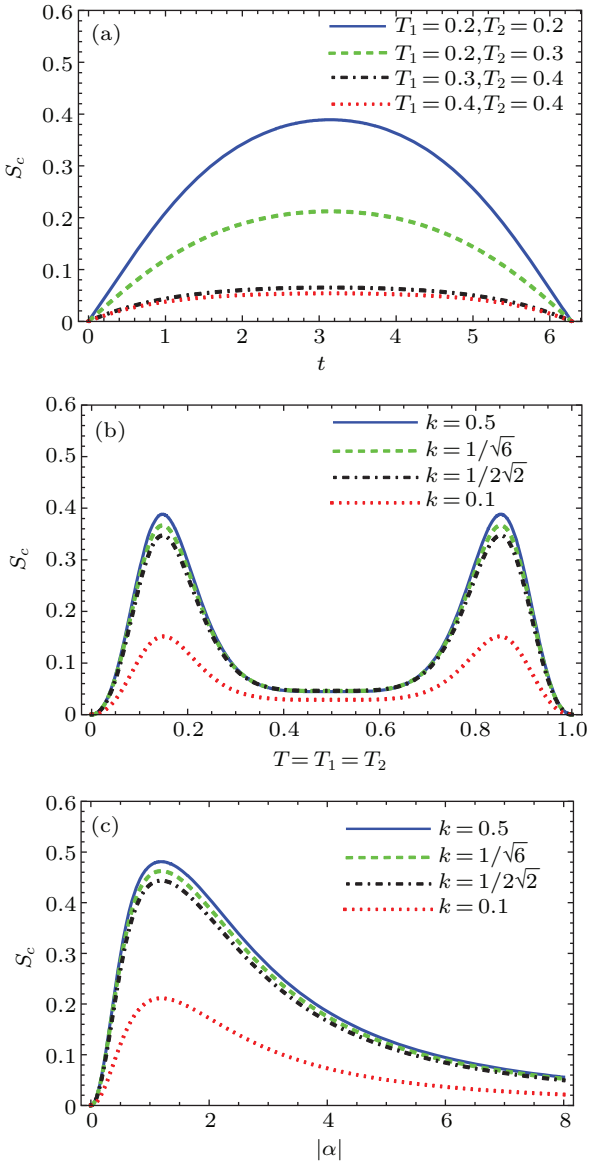


Fig. 5. Linear entropy $S_{\rm c}$ of the cavity mode with operating quantum scissor (a) as a function of time t for several different transmissivities T_1 and T_2 with $|\alpha| = 0.5$, $k = 0.5$ and the initial number state $|1\rangle_{\rm m}$, (b) as a function of transmissivities $T = T_1 = T_2$ for several different parameter k with $|\alpha| = 0.5$ and the initial number state $|1\rangle_{\rm m}$ when $t = \pi/2$, (c) as a function of amplitude $|\alpha|$ for several values of k with $T_1 = T_2 = 0.2$ and the initial number state $|1\rangle_{\rm m}$ when $t = \pi/2$.

Similarly, the linear entropy $S_{\rm c}$ after operating quantum scissor is also plotted in Fig. 5 for several different cases, which shows that quantum scissors can effect the degree of entanglement between the cavity field and the mechanical oscillator. From Fig. 5(a), we see that for a given $|\alpha|$, k and l,

the degree of entanglement is still symmetrically distributed with $t=\pi$ and the maximum value decreases with the increasing transmissivity T_1 or T_2 under the condition of $T_1<0.5$ and $T_2<0.5$. It is interesting from Fig. 5(b) that for a given time t ($t=\pi/2$) the linear entropy S_c all appears two maximum values symmetrically at $T_1=T_2=0.5$ for several values of k with $|\alpha|=0.5$ and $l=1$, and the lower the value of the parameter k is, the smaller the maximum value is. The initial amplitude dependence of the entanglement is shown in Fig. 5(c) for several values of k at fixed $l=1$ when $t=\pi/2$. It is clear that S_c exists a maximum value at small amplitude $|\alpha|$ range and may be close to zero with the increment of $|\alpha|$. Moreover, in order to understand whether the entanglement is enhanced by quantum scissor, by comparing Eq. (15) with Eq. (13) we may depict the feasibility region for enhancing entanglement in ($|\alpha|$, $T=T_1=T_2$) space in Fig. 6. Namely, if $S_c>S_i$, the entanglement is enhanced in principle, or else it is weakened. It is found that the entanglement by evaluating linear entropy turns out to be enhanced within the small amplitude and the low transmissivity or high transmissivity regions (see Fig. 6). These results further illustrate that the high entanglement between the cavity field and the mechanical oscillator can be achieved by operating quantum scissor.

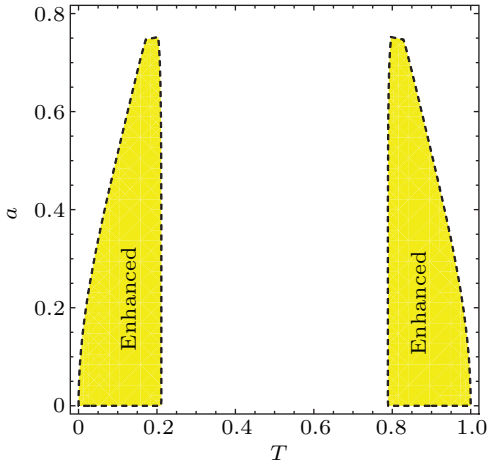


Fig. 6. The feasibility region for enhancing entanglement by evaluating linear entropy S_c of the cavity mode in ($|\alpha|$, $T=T_1=T_2$) space with $k=0.5$ and the initial number state $|1\rangle_m$ when $t=\pi/2$.

5. Wigner function

In the above section, to evaluate the quantum scissor device, we have used fidelity to quantify how close the output state and the input state are. However, fidelity is just a single number and does not give the complete information.[42] Next, we turn our attention to the WF of the output state as a tool which can give complete information on the phase and amplitude of this state. In addition, the negative values in WF are an indicator of the nonclassical property of a state.[47,48]

Firstly, for a given density operator of Fock states, $\rho_{nm}=|n\rangle\langle m|$, using the Wigner function in the coherent state representation $|z\rangle$[49,50]

$$W(\beta)=\frac{\mathrm{e}^{2|\beta|^2}}{\pi}\int\frac{\mathrm{d}^2z}{\pi}\langle -z|\rho|z\rangle\,\mathrm{e}^{-2(z\beta^*-z^*\beta)}, \tag{21}$$

and the expression form of Fock states in the un-normalized coherent state representation ($\|\gamma\rangle=\exp\left(\gamma a^\dagger\right)|0\rangle$)

$$\begin{aligned}|n\rangle&=\frac{1}{\sqrt{n!}}\frac{\partial^n}{\partial\gamma^n}\|\gamma\rangle|_{\gamma=0},\\ \langle m|&=\frac{1}{\sqrt{m!}}\frac{\partial^m}{\partial\eta^{*m}}\langle\eta\||_{\eta^*=0},\end{aligned} \tag{22}$$

we may calculate $W_{n,m}(\beta)$ by

$$\begin{aligned}W_{n,m}(\beta)&=\frac{\mathrm{e}^{-2|\beta|^2}}{\pi\sqrt{n!m!}}\frac{\partial^{n+m}}{\partial\gamma^n\partial\eta^{*m}}\mathrm{e}^{-\gamma\eta^*+2\beta^*\gamma+2\beta\eta^*}|_{\gamma=\eta^*=0}\\&=\frac{\mathrm{e}^{-2|\beta|^2}}{\pi\sqrt{n!m!}}H_{n,m}(2\beta^*,2\beta),\end{aligned} \tag{23}$$

where $H_{n,m}(x,y)$ is two-variable Hermite polynomials with

$$H_{n,m}(x,y)=\frac{\partial^{n+m}}{\partial\gamma^n\partial\eta^{*m}}\mathrm{e}^{-\gamma\eta^*+x\gamma+y\eta^*}|_{\gamma=\eta^*=0}.$$

When $m=n$, $W_n(\beta)=(-1)^m\frac{\mathrm{e}^{-2|\beta|^2}}{\pi}L_m\left(4|\beta|^2\right)$ is just the Wigner function of Fock state $|n\rangle$, where $H_{m,m}(x,y)=(-1)^m m!L_m(xy)$.

Then, based on the results of Eqs. (18) and (23), we may obtain the analytical expression of WF for the cavity mode after operating quantum scissor, i.e.,

$$\begin{aligned}W_o(\beta)&=\frac{1}{p_s}\{\kappa_{00}W_{0,0}(\beta)+\kappa_{11}W_{1,1}(\beta)+\kappa_{22}W_{2,2}(\beta)\\&\quad+2\mathrm{Re}[\kappa_{01}W_{0,1}(\beta)+\kappa_{02}W_{0,2}(\beta)\\&\quad+\kappa_{12}W_{1,2}(\beta)]\}.\end{aligned} \tag{24}$$

When the mirror returns to its original state, namely, $t=2\pi$, the WF of the output state in Eq. (10) for the cavity mode yields

$$\begin{aligned}W'_o(\beta)&=\frac{\mathrm{e}^{-|\alpha|^2}}{p_s}\left\{4\Gamma_0^2W_{0,0}(\beta)-4\Gamma_0\Gamma_1\cos\left(2\pi k^2\right)\mathrm{Re}\left[\alpha W_{1,0}(\beta)\right]\right.\\&\quad+|\alpha|^2\Gamma_1^2W_{1,1}(\beta)+4\sqrt{2}\Gamma_0^2\cos\left(8\pi k^2\right)\mathrm{Re}[\alpha^2W_{2,0}(\beta)]\\&\quad\left.+2|\alpha|^4\Gamma_0^2W_{2,2}(\beta)-2\sqrt{2}\Gamma_1\Gamma_0|\alpha|^2\cos\left(6\pi k^2\right)\mathrm{Re}[\alpha W_{2,1}(\beta)]\right\},\end{aligned} \tag{25}$$

which is just the WF of multicomponent cat states depending on the value of the parameter k. That is to say, $k = 1/2, 1/\sqrt{6}$ and $1/\sqrt{8}$ correspond to two-component, three-component and four-component cat states, respectively.

In Fig. 7, we plot the WF distributions of $W_o'(\beta)$ of Eq. (25) in phase space with $\beta = (q + ip)/\sqrt{2}$ for several different transmissivities $T_1 = T_2$ and parameters $k = 0, 1/2, 1/\sqrt{6}$ at fixed $\alpha = 1 + i$, respectively. It is clearly seen that for the given transmissivities $T_1 = T_2 = 0.2$ or 0.3, the negative region of WF gradually increases with the increase of parameters k, which means that three-component cat state exists the stronger noclassicality than two-component cat state. On the other hand, in comparison of Fig. 7(a) with Fig. 7(d), the structure of WF will be affected by the transmissivities $T_1 = T_2$, which leads to the generation of quantum states with the stronger nonclassical properties via quantum scissors device. In a word, by modulating the transmissivities and parameters k, the negative volume of the WF can be realized and enhanced.

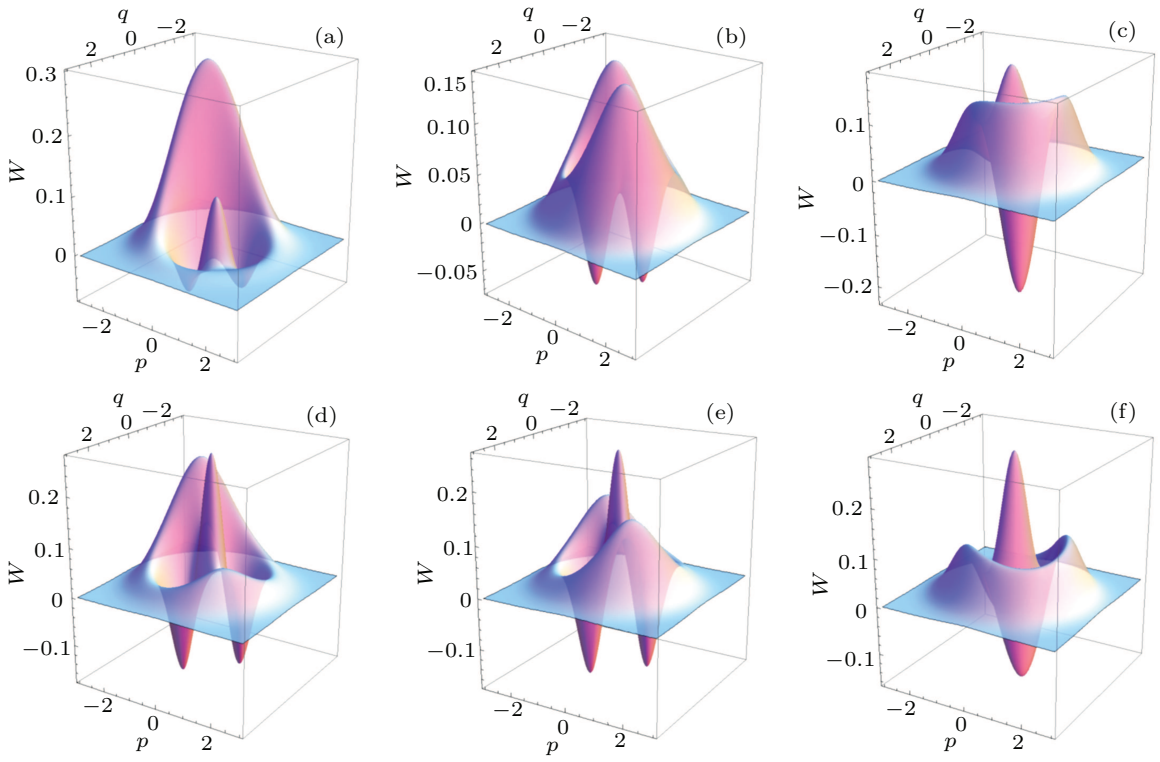


Fig. 7. Wigner function distribution $W_o'(\beta)$ of the output state in phase space with $\beta = (q+ip)/\sqrt{2}$ for several different cases at fixed $\alpha = 1+i$, where we actually consider the multicomponent cat states for the output mode at time $t = 2\pi$ due to dynamics alone. (a) $T_1 = T_2 = 0.2$, $k = 0$, (b) $T_1 = T_2 = 0.2$, $k = 1/2$, (c) $T_1 = T_2 = 0.2$, $k = 1/\sqrt{6}$, (d) $T_1 = T_2 = 0.3$, $k = 0$, (e) $T_1 = T_2 = 0.3$, $k = 1/2$, (f) $T_1 = T_2 = 0.3$, $k = 1/\sqrt{6}$.

6. Conclusions

In summary, we have studied theoretically the influence of the non-classical states generated by QSD operation on the the cavity mode of an optomechanical system, where the cavity field is initially in a coherent state and the mechanical resonator is in a number state. It is found that at time $t = 2\pi$ the mirror recovers its original state and the cavity field returns to a variety of multicomponent cat states by adjusting the value of the parameter k. When QSD with two single photons inputs and two single-photon detections act on the cavity mode of the optomechanical system, the resulted state in Eq. (6) contains only the vacuum, single-photon and two-photon states depending upon the parameter k as well as the transmission coefficients of BSs. We have discussed the success probability of such a state, which all decreases with the increasing amplitude $|\alpha|$ and the curves are symmetric about $T_2 = 0.5$ for a given $|\alpha|$ and T_1 with the corresponding maximum value increasing with the increment of T_1 ($T_1 < 0.5$). In addition, the fidelity between the output state and input state via QSD can be close to 1 for a small amplitude $|\alpha|$ for given transmissivities T_1 and T_2 and monotonously decreases with the increasing $|\alpha|$ for a high transmissivity T_2, which indicates that QSD operation can regulate features of optomechanical states. Then we mainly pay attention to investigating the entanglement between the two subsystems by evaluating linear entropy. It turns out that QSD operation can enhance their entanglement degree and the enhanced region is located at the small amplitude and the low transmissivity or high transmissivity regions. Furthermore, we also derive the analytical expression of WF for the cavity mode via QSD and numerically discuss the WF distribution in phase space at time $t = 2\pi$. The results show that the negative region of WF gradually increases with the increase of

parameters k, which means that three-component cat state exists the stronger noclassicality than two-component cat state. Our work further demonstrates that the optomechanical system with QSD operation is an efficient method in manipulating the nonclassical state, which may become an important source in quantum optics and quantum information processing.

Acknowledgements

Project supported by the National Natural Science Foundation of China (Grant No. 11704051), the Qinglan Project of the Jiangsu Education Department and the Research Foundation of Six Talents Peaks Project in Jiangsu Province, China (Grant No. XNY-093).

References

[1] Dell'Anno F, De Siena S and Illuminati F 2006 *Phys. Rep.* **428** 53
[2] Blatt R, Milburn G J and Lvovsky A 2013 *J. Phys. B: At. Mol. Opt. Phys.* **46** 100201
[3] Kim M S 2008 *J. Phys. B: At. Mol. Opt. Phys.* **41** 133001
[4] Agarwal G S and Tara K 1991 *Phys. Rev. A* **43** 492
[5] Zavatta A, Parigi V and Bellini M 2007 *Phys. Rev. A* **75** 052106
[6] Wang X B, Kwek L C, Liu Y and Oh C H 2001 *J. Phys. B: At. Mol. Opt. Phys.* **34** 1059
[7] Meng X G, Wang Z, Fan H Y, Wang J S and Yang Z S 2012 *J. Opt. Soc. Am. B* **29** 1844
[8] Hu L Y and Zhang Z M 2013 *J. Opt. Soc. Am. B* **30** 518
[9] Biswas A and Agarwal G S 2007 *Phys. Rev. A* **75** 032104
[10] Meng X G, Wang Z, Fan H Y and Wang J S 2012 *J. Opt. Soc. Am. B* **29** 3141
[11] Xu X X, Hu L Y and Fan H Y 2009 *Mod. Phys. Lett. A* **24** 2623
[12] Lee S Y, Park J, Ji S W, Raymond Ooi C H and Lee H W 2009 *J. Opt. Soc. Am. B* **26** 1532
[13] Lee S Y and Nha H 2010 *Phys. Rev. A* **82** 053812
[14] Li H M, Xu X X, Yuan H C, Wang Z, Wan Z L and Xu X F 2015 *Opt. Commun.* **354** 291
[15] Navarrete-Benlloch C, García-Patrón R, Shapiro J H and Cerf N J 2012 *Phys. Rev. A* **86** 012328
[16] Lee S Y, Ji S W, Kim H J and Nha H 2011 *Phys. Rev. A* **84** 012302
[17] Yang Y and Li F L 2009 *Phys. Rev. A* **80** 022315
[18] Guo Y, Liao Q, Wang Y J, Huang D, Huang P and Zeng G H 2017 *Phys. Rev. A* **95** 032304
[19] Ouyang Y, Wang S and Zhang L J 2016 *J. Opt. Soc. Am. B* **33** 1373
[20] Pegg D T, Phillips L S and Barnett S M 1998 *Phys. Rev. Lett.* **81** 1604
[21] Ozdemir S K, Miranowicz A, Koashi M and Imoto N 2001 *Phys. Rev. A* **64** 063818
[22] Miranowicz A, Ozdemir S K, Bajer J, Koashi M and Imoto N 2007 *J. Opt. Soc. Am. B* **24** 379
[23] Miranowicz A 2005 *J. Opt. B: Quantum Semiclass. Opt.* **7** 142
[24] Seshadreesan K P, Krovi H and Guha S 2019 *Phys. Rev. A* **100** 022315
[25] Wang M H and Yan G A 2019 *Chin. Phys. B* **28** 030302
[26] Ren G, Yu H J, Zhang C Z and Zhang W H 2021 *Phys. Scr.* **96** 095103
[27] Ferreyrol F, Barbieri M, Blandino R, Fossier S, Tualle-Brouri R and Grangier P 2010 *Phys. Rev. Lett.* **104** 123603
[28] Babichew S A, Ries J and Lvovsky A I 2003 *Europhys. Lett.* **64** 1
[29] Koniorczyk M, Kurucz Z, Gábris A and Janszky J 2000 *Phys. Rev. A* **62** 013802
[30] Zhao H X, Xu X X and Yuan H C 2017 *Opt. Commun.* **382** 127
[31] Xu X X, Hu L Y and Liao Z Y 2018 *J. Opt. Soc. Am. B* **35** 174
[32] Zhang K Z, Hu L Y, Ye W, Liu C J and Xu X X 2019 *Laser Phys. Lett.* **16** 015204
[33] Liu C J, Yu M, Ye W, Zhang H and Hu L Y 2020 *Results Phys.* **19** 103616
[34] Ghalaii M, Ottaviani C, Kumar R, Pirandola S and Razavi M 2020 *IEEE J. Sel. Top. Quantum Electron.* **26** 6400212
[35] Li H M, Xu X X, Huang H Y, Wang Z, Wan Z L and Yuan H C 2020 *J. Opt. Soc. Am. B* **37** 1054
[36] Aspelmeyer M, Kippenberg T J and Marquardt F 2014 *Rev. Mod. Phys.* **86** 1391
[37] Liao J Q and Tian L 2016 *Phys. Rev. Lett.* **116** 163602
[38] Sekatski P, Aspelmeyer M and Sangouard N 2014 *Phys. Rev. Lett.* **112** 080502
[39] Jiang L Y, Guo Q, Xu X X, Cai M, Yuan W and Duan Z L 2016 *Opt. Commun.* **369** 179
[40] Liang X Y, Guo Q and Yuan W 2019 *Int. J. Theor. Phys.* **58** 58
[41] Mancini S, Man'ko V I and Tombesi P 1997 *Phys. Rev. A* **55** 3042
[42] Bose S, Jacobs K and Knight P L 1997 *Phys. Rev. A* **56** 4175
[43] Yang T L, Zhu C L, Liu S and Xu Y J 2021 *Chin. Phys. B* **30** 124201
[44] Shi H and Bhattacharya M 2013 *Phys. Rev. A* **87** 043829
[45] Hu L Y, Xu X X, Wang Z S and Xu X F 2010 *Phys. Rev. A* **82** 043842
[46] Zurek W H, Habib S and Paz J P 1993 *Phys. Rev. Lett.* **70** 1187
[47] Kenfack A and Życzkowski K 2004 *J. Opt. B: Quantum Semiclass. Opt.* **6** 396
[48] Tan K C, Choi S C and Jeong H 2020 *Phys. Rev. Lett.* **124** 110404
[49] Fan H Y 2003 *J. Opt. B: Quantum Semiclass. Opt.* **5** R147
[50] Wünsche A 1999 *J. Opt. B: Quantum Semiclass. Opt.* **1** R11